Open Access
Volume 6 Issue 3
Research Article

Journal of Water Engineering and Management
ISSN: 2582-6298

Hydraulic Analysis of Irrigation Canal Using HEC-RAS Model: A Case Study of Latifshah Weir in Uttar Pradesh, India

Soni Kumari[1*], Mritunjay Kumar[1], Ajai Singh[2]

[1]M. Tech Student, Water Resources Engineering, Dept. of Civil Engineering, Central University of Jharkhand, Ranchi, Jharkhand.

[2]Department of Civil Engineering, Central University of Jharkhand, Ranchi, Jharkhand.

Article Info

Article History:
Received on: August 10, 2025
Revised on: September 10, 2025
Accepted on: December 4, 2025
Published on: December 31, 2025
Published by Academic Hope

***Corresponding author:** Soni Kumari*
Email: sonishalu2508@gmail.com

How to Cite:
Kumari, S., Kumar, M. and Singh, A. 2025. Hydraulic Analysis of Irrigation Canal Using HEC-RAS Model: A Case Study of Latifshah Weir in Uttar Pradesh, India. Journal of Water Engineering and Management, 6(3): 1-13. DOI: https://doi.org/10.47884/jweam.v6i3pp01-13

Abstract

India's expanding population raises the need for water, notably in agriculture, which consumes around 70-80% of the country's water. As competition for water resources intensifies across different sectors, increasing the efficiency of irrigation canal systems that provide water to agricultural crops is important. Improving these systems can assist in saving limited water resources, expanding irrigated areas, and enhancing local stakeholders' socio-economic conditions. In the present study, the HEC-RAS model was applied to analyse the hydraulics of the left Karmanasa canal irrigation system in Uttar Pradesh, India. Hydraulic models are important tools for studying the flow dynamics of open channels. The HEC-RAS model was calibrated and validated to simulate the water depths. The model was tested across a range of Manning's n values from 0.020 to 0.025. The calibrated value was determined to be 0.023. Calibration and validation of the model produced good results at all sites, with Coefficient of Determination (R^2) and Correlation Coefficient (r) values ranging from 0.99 to 0.80 and the value of Nash-Sutcliffe efficiency (NSE) ranged from 0.90 to 0.60. The results can be used for effective water management in canal irrigation systems by reducing losses and operation and maintenance costs.

Keywords: HEC-RAS: Open channel flow: Canal operation and maintenance: Canal capacity: Discharge: Karmanasa canal irrigation.

Introduction

The irrigation canals are essential for carrying water from the source to the agricultural lands. Water is transported from natural sources and directed through delivery networks to the fields as part of the distribution systems. Water losses through conveyance and distribution network of canals must be addressed in order to maximize the water usage efficiency. Increasing the irrigated area and improving the irrigation supply system's efficiency are necessary to meet future needs (Vedmani et al., 2020). Routine maintenance and modernization are reliable ways to improve irrigation canal efficiency. Canal maintenance activities include desilting, vegetation clearing, and repairs, whereas modernization means updating both technical and management components to improve the total irrigation service supplied to farmers. Hydraulic modeling examines and predicts the movement of water in both natural and manmade scenarios, such as rivers, canals, and irrigation systems (Bwambale et al., 2019). These models allow for an assessment of the possible consequences of planned system changes such as dam construction or water diversion for agriculture, water quality and availability. Models may be used to design water control systems and enhance their operating efficiency.

Different models have been used to perform hydraulic evaluations on irrigation canals (Barkhordari and Shahdany, 2022; Kamran et al., 2020). A popular computer tool for hydraulic analysis of irrigation canals and other water courses is the River Analysis System from the Hydrologic Engineering Center (HEC-RAS). The HEC-RAS model has been used in recent research to examine irrigation canal hydraulic performance (USACE, 2016). The HEC-RAS model was effectively utilized in research by Serede et al. (2015) on Kenya's Mwea Irrigation Scheme to assess the hydraulic characteristics of the irrigation system and identify the canal retention ability. Several researchers have worked on analysis of the maximum capacity of Irrigation Scheme (Sargison and Barton, 2008; Clarke et al., 2010; Patamanska and Grancharova, 2019; Kamran et al., 2020; Vedmani et al., 2020; Gilja et al., 2021; Nugroho et al., 2021; Barkhordari and Shahndany, 2022; Abo-Sreeaa et al., 2023; Ontowirjo et al., 2023), predicting floods and flood inundation mapping (Timbadiya et al., 2011; Parhi et al., 2012; Goodell, 2016; Gruss et al., 2018; Ardiclioglu and Kuriqi, 2019) and comparison of HEC-RAS with other models (Mohammed and Qasim, 2012). A thorough understanding of canal hydraulic behaviour may assist in the development of effective strategies to manage water resources. This can lead to a more effective distribution system that preserves water supplies. In the present study, the effects of structural and hydraulic alterations on the reach potential capacity of the Left Karmanasa Canal using the HEC-RAS model has been analysed. The aim is to develop improved operation and maintenance protocols for enhancing the performance of this canal system.

Materials and Methods

Description of Study Area

The district of Chandauli in Uttar Pradesh, India is located between 24° 56′ and 25° 35′ north latitudes and 81° 14′ to 84° 24′ east longitudes. Its boundaries are shared by Sonebhadra District to the south, Bihar to the east, Ghazipur District to the north-northeast, Bihar to the southeast, and Mirzapur to the south-west (Fig. 1). The border between Chandauli and Bihar is the Karmanasa river. The district's landscape and economics are significantly shaped by the Ganga, Karmanasa, and Chandraprabha rivers. Chandauli District comprises five tehsils, namely Sadar, Sakaldiha, Chakia, Mughalsarai, and Naugarh. The district is comprised of nine blocks, namely Barahani, Chandauli, Niyamatabad, Chahaniya, Sakaldiha, Dhanapur, Chakia, Shahabganj, and Naugarh. The district of Chandauli is separated into three zones depending on geology, soils, geography, climate, and natural vegetation, namely Chakia Plateau, Chandauli plain and Ganga Khadar (https://chandauli.nic.in/geography/). The district receives 915.20 mm of rainfall on average every year, with the majority of the rainfall falling between July and September (Fig. 2).

The Karmanasa River rises to a height of 350 meters in the Kaimur district of Bihar, close to Sarodag on the northern side of the Kaimur Range. It finally meets the Ganges close to Chausa after flowing northwest across the plains of Mirzapur and acting as a border between Uttar Pradesh and Bihar. The river is 192 km long; 116 of those km is in Uttar Pradesh, while the final 76 km mark the border between Uttar Pradesh and Bihar. 11,709 km^2 make up the Karmnasa's entire drainage basin, including its tributaries (Jain et al., 2007). Latif Shah weir and Nuagarh dam are two notable dams on the Karmanasa; there is also a dam on the Chandraprabha (Prakash et al., 2019).

Latifshah Weir

The Latifshah Dam, in the Chandauli district, is one of the country's oldest dams. It was constructed in 1921 and is situated on the Karmnasha river. The reservoir generated by the dam is primarily used for agriculture and human consumption. Left Karmanasha Canal originates from Latifshah weir under Chakia of Chandauli district. The total length of this canal is 7.100 km and is connected to the Karmanasha system whose CCA is 35221 hectares. Chandauli main canal emerges from the tail of this canal, whose length is 47.800 km (Uttar Pradesh Irrigation and Water Resource Department, 1823).

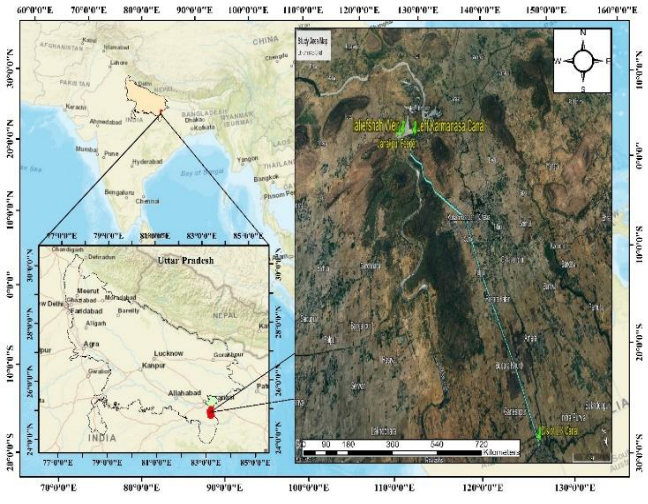

Fig. 1 Study area map

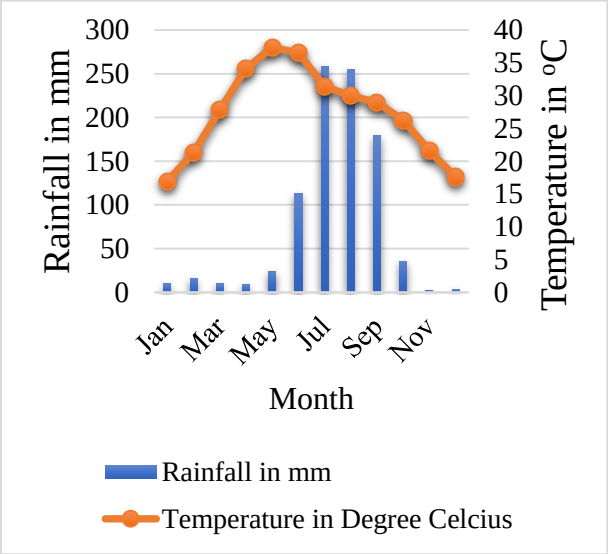

Fig. 2 Mean monthly rainfall and temperature data (https://indiawris.gov.in/wris/#/rainfall, https://power.larc.nasa.gov/data-access-viewer/)

Detailed information about the construction features and storage capacities of the Latifshah Weir is provided in Table 1 and Table 2, along with some important salient features of the site and details about the controlling organization responsible for its management. Figure 3 (a) shows the starting point of the canal channel originating from the Latifshah Weir. Figure 3 (b) captures a dip in the canal located 6 km downstream (referred to as point D2) from the canal's upstream section. At this location, a Village Road Bridge (VRB) has been constructed over the canal. Fig. 3 (c) displays a newly installed device used to measure the depth of flow (noted as D_{obs}, in meters or feet) and the corresponding discharge value (noted as Q_{obs}, in cumecs or cusecs). Previously, these measurements were taken using direct methods, such as canal gauges - markings placed along the canal banks that indicate the water level. These gauges allowed for simple, manual readings of water depth

Table 1 Constructional features and storage capacities (Uttar Pradesh Irrigation and Water Resource Department, Chandauli)

Water catchment area	7770 ha
Water storage capacity of the dam	350 million cubic feet (mcft)
Dead storage capacity of dam	100 million cubic feet (mcft)
Maximum flood discharge	130810 cusecs (3706 cumecs)
River Sluice	1 no. 3× 4 feet size
Sluice of canal gate	Left Karmanasa Canal- 2 no. 10×5 and 6×5 feet size, Right Karmanasa Canal- 2 no. 8×8 feet size Janakpur feeder- 1 no. 8×8 feet size
Crest Length	185.73 m
Crest width	4.27 m
Crest Height	87.55 m
Flood discharge sill level	81.30 m
Sill level of river sluice	73.89m
Sill level of Left Karmanasa canal (gate)	82.91 m
Sill level of Right Karmanasa Canal (Gate)	82.91m
Sill level of Janakpur feeder (gate)	85.95 m
Maximum Description Level	87.55 m
Maximum flood level	92.51 m
Downstream flood level	73.89 ft
Efflux bandh Peak level	93.73 m
Length of Efflux bandh	➢ Left - 4.325 km ➢ Right - 0.140 km
Slope of Dam	U/S and D/S - 2:1

Table 2 Salient features of Latifshah Weir (Uttar Pradesh Irrigation and Water Resource Department, Chandauli)

1	Name of Dam	Latifshah Weir
2	Operated & Maintained By	Civil Organisation
3	Latitude	25^0 01′ 13′′ N
4	Longitude	83^0 14′ 33′′ E
5	Year of completion	1917 to 1922
6	River Basin	Karmanasa River Basin
7	River	Karmanasa River
8	Nearest City	Chakia
9	Seismic Zone	4^{th}
10	Type of Dam	Earthen Dam
11	Heigh above Lowest Foundation(m)	19.84 m
12	Length of Dam	4465 m
13	Volume Content of Dam	254253.73 m^3
14	Gross Storage Capacity	9.92 m^3
15	Reservoir area	7770 ha
16	Effective Storage	9.92 m^3
17	Purpose	Irrigation
18	Designed Spillway Capacity (m^3 /sec)	3706 cumecs

Model Description and Input Data

HEC-RAS is used to calculate the water level profile in one dimension under steady flow. A flow chart of the methodology for applying the HEC-RAS model to accomplish the primary goal of the study is shown in Fig. 4. The HEC-RAS model used discharge, expansion or contraction of flow, channel roughness, energy loss coefficients for hydraulic resistance, and boundary conditions for the canal flow (such as the surface of the lining) as inputs. Cross-sectional geometry collected at regular intervals throughout the study length was also considered. Depending on site-specific factors like the longitudinal uniformity of the cross-sectional shape, the linearity of the channel, the longitudinal slope, and the uniformity of the slope throughout the study reach, the distribution of necessary cross-sections varies from station to station (Serede et al., 2015). The interpolation method was used to create additional cross-sections in order to improve model calibration.

Fig. 3 Left Karmanasa canal site

This was necessary because of a couple of purposes, including the backwater effects of check structures, changes in canal geometry, drop structures, slope modifications, and roughness variations in the canal. To accurately define the slope, cross-sections were placed upstream and downstream of falls and drop structures. In the geometry file, all elevations were entered as absolute values. The Chandraprabha division pt. D.D.U. Nagar, Chandauli provided the canal cross-section geometries at different reach stations, discharge data, slope (S), and side slopes that have been collected for the HEC-RAS model.

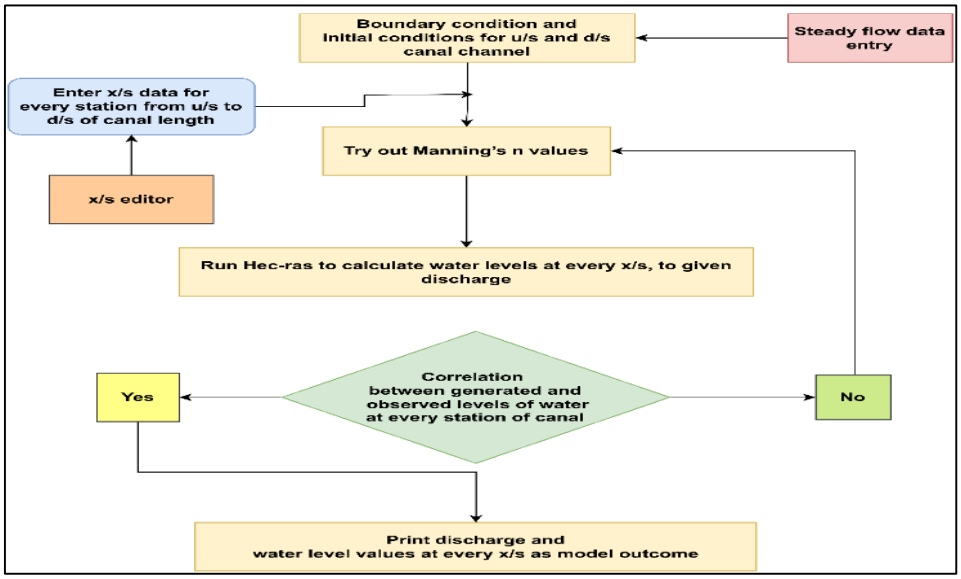

Fig. 4 Flow chart of calibration of HEC_RAS model

Model Calibration and Validation

The canal under study has a trapezoidal cross-section with a bottom width of 12.8 m and side slopes of 2:1. It is designed to carry water at a depth of 2.60 m, with an additional freeboard of 0.90 m for safety. For hydraulic analysis, a Manning's roughness coefficient (n) of 0.022 was initially used. The canal bed has a mild and constant slope of 0.0002, except at two locations where sharp dips occur at 5.30 km (D1) and 6.00 km (D2) downstream. Additional data received from the Chandraprabha Division on January 13, 2024 includes cross-sectional drawings at chainages of 0.750 km, 1.100 km and 6.400 km from the upstream end of the Left Karmanasa Canal. A longitudinal section of the canal with data at 0.200 km intervals includes chainage (km), ground level (GL), old bed level (based on a discharge of 850 cusecs, bed width 30 m, bed slope 0.15 m/km and water depth 2.53 m), new bed level (corresponding to a discharge of 1398 cusecs, bed width 12.8 m, bed slope 0.20 m/km and water depth of 2.60 m).

The HEC-RAS geometry data editor receives this data. The HEC-RAS geometry data editor receives geometry data from each cross-section at the reach stations. Along with main channel bank values that differ between stations, each station entry specifies a downstream length of 200, 100, or 50 meters. For every reach station, 0.1 and 0.3 contraction and expansion factors are used, respectively. According to Chow's (1959) recommendations for Manning's values, roughness, rugosity, and underbrush severity are taken into consideration while assigning Manning's roughness coefficients, which range from 0.020 to 0.023. The HEC-RAS model for this study was run using a subcritical steady flow analysis. It required entering the boundary conditions, which included discharge and slope data obtained from the reach stations. The hydraulic flow parameters of the Left Karmanasa canal were studied using the HEC-RAS model version 6.5 beta.

The model was calibrated using 8 occurrences which include discharge data and observed water depths recorded from January to July 2023 (Table 3). The calibration technique involved iteratively modifying the Manning's roughness coefficient to ensure that the simulated and observed water depths are within acceptable bounds. The model received cross-sectional data from each station along the canal, from upstream to downstream. Manning's roughness coefficients are determined for each segment. The boundary criteria for the full length of the canal are defined. The simulated water depths are compared to the actual water depths at each location. Iteratively repeating this process continued until the variations

between the simulated and observed water depths satisfied the predetermined standards.

The model is run with various Manning roughness coefficients (n) ranging from 0.020 to 0.025. The model's projected flow depths are then compared to observed flow depths. This comparison yielded the calibrated value of Manning's n, which was 0.0234. It is vital to highlight that in this study, the roughness coefficient has remained constant throughout all cross-sections with no lateral variations. Data of several events during August to October 2023 were selected for the model verification phase (Table 4). Evaluating the correctness of calibrated parameters is a step in the validation of the model. In order to verify the model, fresh simulated water depth data are compared with the real water depth measurements in order to assess the correctness of the calibrated parameter, Manning's 'n'.

Table 3 Measured and simulated depth hydrographs for different values of the roughness coefficient.

Measured Data (Discharge data i.e. $Q_{obs.}$ (m^3/s) and depth i.e. $d_{obs.}$ (m)) of Canal was taken b/w Jan,2023 to Jul 2023. (used to calibrate the model firstly).	Q_{in} (m^3/s)	$d_{obs.}$ (m)	$d_{sim.}$ (m) (Simulated depth)		
	Observed (Q) & Depth (d)		n=0.020	n=0.022	n=0.0234
	3.20	0.6	0.55	0.58	0.6
	5.80	0.85	0.79	0.83	0.85
	6.50	0.91	0.84	0.89	0.91
	8.50	1.07	0.99	1.04	1.07
	14.60	1.46	1.35	1.43	1.46
	15.60	1.52	1.40	1.48	1.52
	16.20	1.55	1.43	1.51	1.55
	17.60	1.62	1.50	1.59	1.62

Measured Data (Discharge data i.e. $Q_{obs.}$ (m^3/s) and depth i.e. $d_{obs.}$ (m)) of Canal was taken b/w Aug,2023 to Oct,2023. (used to validation the model finally).	Q_{in} (m^3/s)	$d_{obs.}$ (m)	$d_{sim.}$ (m) (Simulated depth)
	Observed (Q) & Depth (d)		n=0.0234
	2.07	2.07	2.07
	2.04	2.04	2.04
	2.01	2.01	2.01
	1.98	1.98	1.98
	23	1.89	1.89
	22.80	1.88	1.88
	16.80	1.58	1.58
	15.10	1.49	1.49

Table 4 Hydrographs of observed discharge data and depth time series for the month of July 2023 measured at the u/s of the canal using Direct Gauge method.

Sl. No.	Date of measurement	Observed discharge (m^3/s) at u/s	Observed depth of flow (m) at u/s
1.	13th July 2023	1.24	0.60
2.	14th July 2023	1.24	0.60
3.	15th July 2023	4.10	1.22
4.	16th July 2023	4.10	1.22
5.	17th July 2023	4.10	1.22
6.	18th July 2023	4.10	1.22
7.	19th July 2023	2.97	0.91
8.	20th July 2023	2.97	0.91
9.	21th July 2023	2.97	0.91
10.	22th July 2023	5.87	1.52
11.	23th July 2023	5.87	1.52
12.	24th July 2023	5.87	1.52
13.	25th July 2023	4.10	1.22
14.	26th July 2023	4.10	1.22
15.	27th July 2023	4.10	1.22
16.	28th July 2023	4.10	1.22

Model Performance and Evaluation

The agreement between modelled and observed data is evaluated using the coefficient of determination (R^2) and Pearson's correlation coefficient (r) and Nash-Sutcliffe coefficient (NSE). The intensity and direction of a linear relationship are indicated by the correlation coefficient, which runs from -1 to 1. A linear correlation is absent when the r value is equal to 0, while perfect positive or negative linear

correlations are represented by r values of 1 or -1, respectively. Conversely, R^2 denotes the proportion of variance in the observed data that can be predicted by the model; its values fall between 0 and 1.

A strong match between the model predictions and the actual data is typically indicated by a higher R^2, especially values over 0.5 (Santhi et al., 2001). However, according to Moriasi et al. (2007), both r and R^2 may be extremely sensitive to outliers and may not be sufficient to explain systematic differences in magnitude or location between predicted and actual values. The Nash-Sutcliffe Efficiency (NSE) factor was developed by Nash and Sutcliffe to assess model performance (Nash and Sutcliffe, 1970). The formula is similar to the R^2 value in linear regression, except it may be used directly to the original data in any model. Unlike R^2, the Nash-Sutcliffe Efficiency (NSE) can range from -∞ to 1. Typically, researchers want an NSE value close to 1. A negative NSE indicates the model performs poorly. NSE is a commonly used metric of model effectiveness in hydrology and other domains (Moriasi et al., 2007).

Nash-Sutcliffe efficiency (NSE)

$$NSE = 1 - \frac{\sum_{i=1}^{n}(d_{oi} - d_{si})^2}{\sum_{i=1}^{n}(d_{oi} - d_o)^2} \quad \dots (1)$$

Pearson's correlation coefficient (r)

$$r = \frac{\sum_{i=1}^{n}(d_{oi} - d_o)(d_{si} - d_s)}{\sqrt{\sum_{i=1}^{n}(d_{oi} - d_o)^2 \sum_{i=1}^{n}(d_{si} - d_s)^2}} \quad \dots (2)$$

Coefficient of determination (R^2)

$$R^2 = (r)^2 \quad \dots (3)$$

where,

n = Total number of observations

d_{oi} = Observed depth of water for the i^{th} point of station

d_o = Average of observed water depth values

d_{si} = Simulated depth of water for the i^{th} point of station

d_s = Average of simulated water depth values

A visual means of comparing simulated and observed constituent data is provided by graphic approaches, which may be used as a preliminary measure of the efficacy of a model (ASCE, 1993; Moriasi et al., 2007). The significance of graphical tools for appropriate model evaluation is emphasized by (Legates and McCabe,1999). Hydrographs and likelihood curves for % exceedance are common examples of graphical tools.

Results and Discussion

The geometry data was entered into the HEC-RAS geometry plan for this simulation. The Manning's n values were kept at 0.020, 0.022, and 0.023 in sequential order. For the steady flow data, a downstream boundary condition with a bed slope of 0.0020 was chosen. The model was run and the water surface profile, velocity profile, and depth were recorded. Furthermore, a full output table offers a thorough understanding of the parameters. For the Manning's n value of 0.023, the simulated depth completely matched the design depth. It is evident that as the channel goes from u/s to d/s, there is decrease in the depth in the direction of flow gradually (Fig. 5). As it approaches to the location of bed dips, there is fluctuation in the depth in order of decrease to increase as it goes in d/s. which results in excessive difference between the value of depth at u/s and d/s as in comparison of bed dip location. HEC-RAS model was calibrated and validated for simulation of depth of water at downstream side for different discharges as mentioned in Table 4. Observed versus simulated water depth for canal discharge of 14 m^3/s is shown in Fig. 6. The model performance was evaluated during calibration period with the r, NSE and R^2. The R^2 values in most of the cases were found more than 0.90 and NSE was found to be in the range of 0.90 to 0.60. This indicates that the model performed well in simulating the water depth. For the model validation phase, data from eight events-based on canal flow measurements collected from the site between August and October 2023 were selected. To validate the model, new simulated water depths were generated using the calibrated parameters. These simulated values were then compared with the actual measured water depths from the field. This comparison helped confirm whether the model, with the calibrated Manning's 'n', could accurately reproduce real-world flow conditions. The model performed well with the validation data set (Table 5).

Table 5 Model's performance statistics during calibration of simulated depth of water

Discharge at inlet of canal, Q_{in} (m^3/s)	r	R^2	NSE
3.20	0.96	0.93	0.84
5.80	0.97	0.95	0.81
6.50	0.98	0.96	0.79
8.50	0.91	0.84	0.71
10.6	0.91	0.84	0.69

14	0.95	0.91	0.77
14.60	0.95	0.90	0.73
15.60	0.94	0.89	0.66
16.20	0.94	0.90	0.67
17.60	0.97	0.94	0.79

Table 6 Model's performance statistics during validation of simulated depth of water

Discharge at inlet of canal, Q_{in} (m^3/s)	r	R^2	NSE
27.20	0.98	0.97	0.86
26.50	0.98	0.96	0.82
25.80	0.96	0.92	0.73
25	0.95	0.90	0.67
23	0.97	0.94	0.79
22.80	0.95	0.90	0.70
19	0.98	0.96	0.87
16.80	0.98	0.97	0.85
15.10	0.95	0.91	0.71
13.50	0.97	0.95	0.68

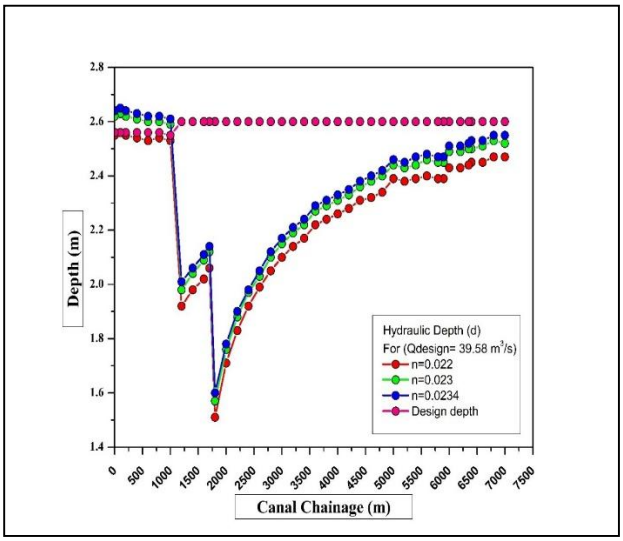

Fig. 5 Simulated and measured water depth along the canal for Q=39.59 m^3/s at n=0.020, 0.022 and 0.023

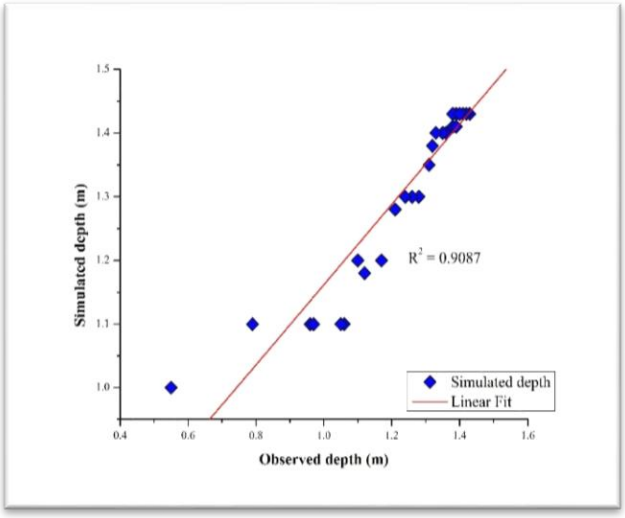

Fig. 6 Observed versus simulated water depth for canal discharge of 14 m^3/s

Substantially, there is loss of potential carrying capacity of canal approximately 20-50% at the dips in bed. The cross-section shown in Fig. 7 shows the range of water levels that are seen in relation to the various discharge data values that are derived from the data that was gathered during the irrigation months of August to October, 2023. It depicts the trapezoidal shape of the canal, which has a side slope of 2:1 and a bottom width of 12.8 m. The canal has a freeboard of 0.90 m and a design depth of 2.60 m. Using a Manning's roughness coefficient (n) value of 0.023 for this channel, the measured depths at the upstream (u/s) and downstream (d/s) parts of the canal are evaluated during validation. The water surface profile for the whole length of the canal under consideration is shown in Fig. 8. The canal bed has a constant, mild 0.0002 slope, with the exception of two sharp dips that happen 5.30 km and 6.00 km downstream. The canal under consideration for study has a total length of 7.10 km. The ground profile of the canal is mostly earthen and shows little variation. The Fig. 8 shows the critical depths determined by HEC-RAS's steady flow analysis, as well as the observed water surface levels that correlate to the different flow data points during validation. The water depth profiles are consistent throughout the canal system, with the exception of dips in the bed level. Water depth variations may be seen clearly along the canal from upstream to downstream, both in terms of simulated and actual data.

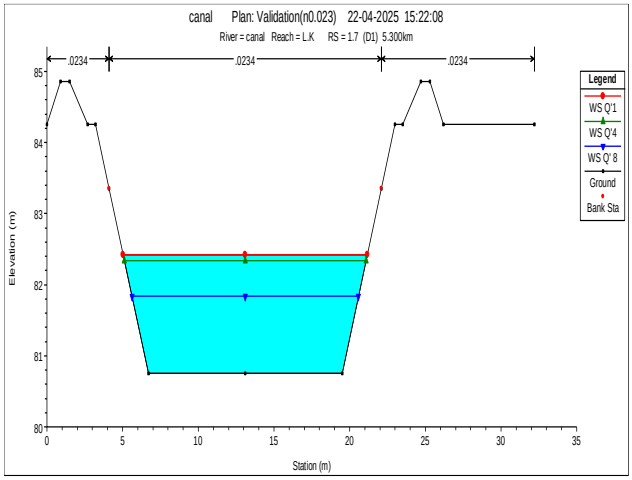

Fig. 7 Canal cross-section plot for roughness coefficient n=0.0234 and various discharge events during the validation of the model

Fig. 9 shows the plot of velocity profile at various discharge events. It is observed that as the flow approaches from u/s to d/s direction, there is gradual increase in velocity up to 5.30 km station reach and then at the bed dip of 5.30 km and at 6.00 km, there is sudden drop in velocity observed at both dip locations. It regains their velocity as it goes further in d/s. Under the steady flow assumption, the starting velocity stays relatively modest, with the exception of the canal's head reach. This is where the water needed for irrigation comes from the reservoir upstream of the weir, which is controlled by gates at the head that may be opened manually or mechanically. By acting as barriers, these gates control and guide the water that is retained for irrigation. The flow velocity rises as it gets closer to two dips in the canal bed. Nonetheless, the velocity decreases at certain locations due to the abrupt reduction in bed levels, assuring a continuous steady and controlled flow movement. By constructing dips at certain points, these fluctuations in velocity are mitigated and the degradation of the earthen canal caused by high velocity rates can be prevented. The increased velocity may alter the canal's shape and bed, thus it's important to maintain steady-state conditions to ensure that the sufficient irrigation water is continuously supplied over a long period of time. In order to do this, proper operation and maintenance are essential.

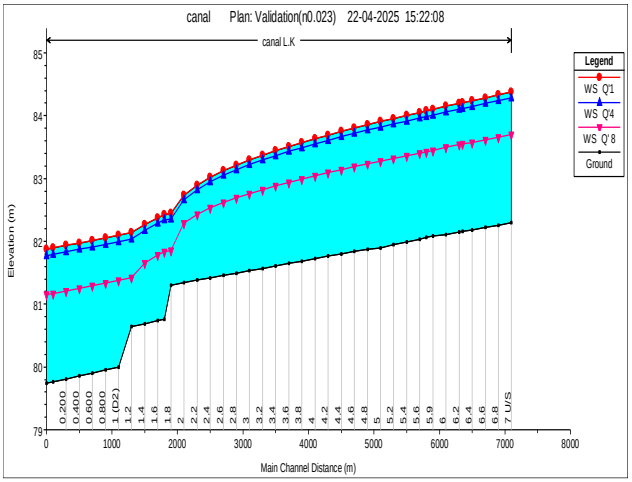

Fig. 8 Water surface profiles of the canal

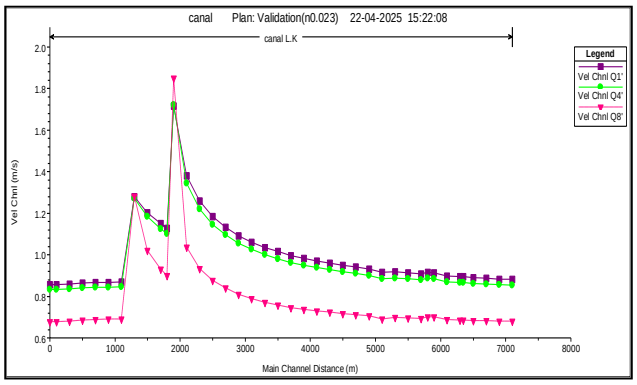

Fig. 9 Velocity profile of the channel during validation of model at n=0.0234

During each discharge validation operation, significant variations in hydraulic depths along the channel are detected as shown in Figure 10. This figure shows the kind and pace of decline. In this case, the simulated depth is greater upstream and at the most downstream location. However, it steadily declines in the direction of flow, with the most substantial reduction occurring at two bed dip places. Beyond these places, depth gradually increases towards the canal system's tail end, which is consistent with observed and simulated depths at upstream and downstream locations in the canal reach. The model's performance is considered good, as seen by R^2 and r values ranging from 0.99 to 0.80 across the various flow profiles. NSE also ranges b/w 0.90 to 0.60, which means that the model is perfectly fit in terms of simulation and performance.

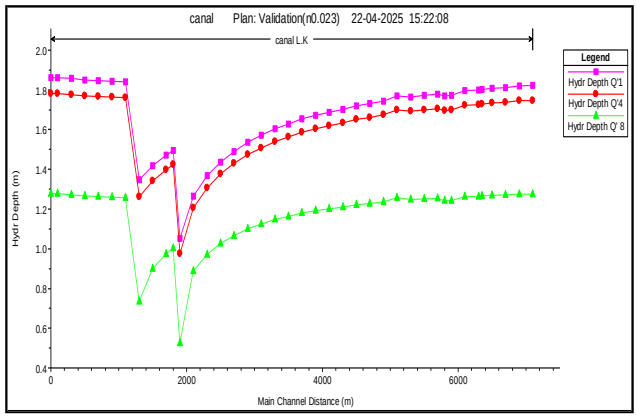

Fig. 10 Variations in hydraulic depth along the channel at the time of validation

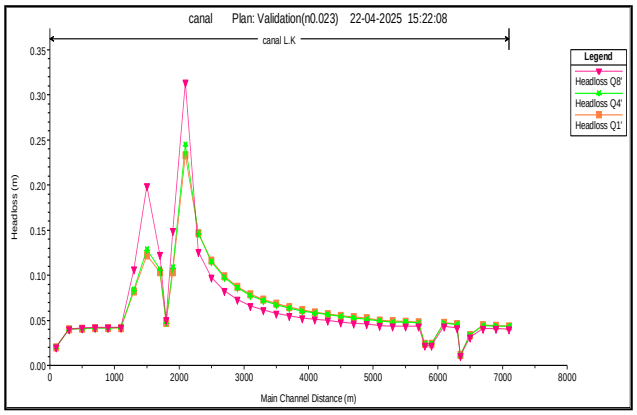

Fig. 11 Head loss at every location of canal section for various discharges events considerate for validation

Head loss in canal sections plays an important role in the design and operation of irrigation systems, water delivery networks, and drainage canals. Friction and other resistances cause head loss when water travels through the canal, which reduces the efficiency and capacity of the water supply. The Figure 11 displays head loss at several locations in a canal section during various flow events. Factors causing head losses are described based on discharge rate, canal geometry, and surface roughness, water depth, obstructions and vegetation, impact of different discharge events, location-based circumstances. Slower velocities near the canal's beginning result in less head loss in upstream sections. Entry conditions as well as initial roughness are two variables to consider. Downstream sections have the most head loss due to the frictional forces that accumulate along the canal. Exit structures and endpoint characteristics are an instance of downstream situations that influence ultimate head loss values. Understanding head loss at various locations in a canal during different discharge events is critical for effective water management. Engineers may construct and maintain canals to reduce head loss by taking into account elements such as discharge rate, canal geometry, and surface roughness, resulting in optimal performance of water distribution systems.

Conclusions

The aim of this research was to evaluate the influence of hydraulic and structural changes on the potential capacity of the Left Karmanasa canal reach in Chandauli district of Uttar Pradesh, India, as well as to design improved operating and maintenance plans for the system, using the HEC-RAS model as a decision support tool. This includes calibrating the model with a focus on maximizing the roughness coefficient, which has been recognized as a crucial parameter. Relevant physical and conceptual parameters are obtained from the Irrigation Department of the state and determined by using existing procedures. The HEC-RAS model's performance was assessed using statistical and graphical approaches to prove its efficacy. The following conclusions can be drawn from the study:

i. Based on daily event-based discharge data for 2023, the Manning's roughness coefficient, which is the only calibration and validation parameter utilized in the HEC RAS model for the Left Karmanasa canal, was found to be 0.0234.

ii. Statistical metrics such as the correlation coefficient (r), coefficient of determination (R^2) and Nash-Sutcliffe efficiency (NSE) are used to evaluate the model's effectiveness. The near agreement between the simulated and observed water depths indicate the effectiveness of the model.

iii. The analysis revealed significant fluctuations in depth, velocity, and discharge, particularly near the channel bed drops. Two distinct

drop locations, Dip D1 and Dip D2, caused a substantial reduction in carrying capacity ranging from 20% to 50% at these spots. While the parameters functioned well at both the start and end of the canal segment, instabilities were observed near the drop points.

iv. drop locations, Dip D1 and Dip D2, caused a substantial reduction in carrying capacity ranging from 20% to 50% at these spots. While the parameters functioned well at both the start and end of the canal segment, instabilities were observed near the drop points.

v. It is recommended to line the canal in order to preserve its structural integrity and increase its capacity. To maintain lifespan, regular short and long-term maintenance should be prioritized, with an emphasis on the canal's banks and bed.

Limitation of the Study and Future Scope

Water losses from evaporation and seepage are not presently taken into account by the HEC-RAS model. As a result, new techniques must be used to evaluate these losses. Subsequent studies have to concentrate on creating strategies that combine the HEC-RAS model's capabilities with techniques for calculating water losses through evaporation and seepage. Extending this model to assess downstream canal performance would help develop comprehensive water management strategies and ensure equitable distribution of water, especially during the dry season.

Significance of the Study for Field Engineers

This study offers significant insights for field engineers and decision-makers in the Uttar Pradesh Irrigation Department, especially those involved in the planning, operation, and maintenance of the Left Karmanasa Canal and its associated network. By using the HEC-RAS hydraulic model, the study has successfully demonstrated how hydraulic and structural factors affect the canal's water-carrying capacity. Field engineers can now better understand the impact of channel deformations, mild bed slopes, and unlined sections on the canal's overall performance. The study also highlights the need for regular inspections and maintenance, especially near areas of structural weakness, like canal dips and unlined sections. This guidance is particularly valuable for on-site engineers who are responsible for maintaining canal performance and ensuring efficient water delivery.

Acknowledgement

The authors wish to express their sincere thanks to Aparajita Singh (A.E.), Rakesh Tiwari (A.E.), Maniraj Singh Yadav (J.E.), and Dhirendra Kumar Tiwari (Senior Water Account Assistant) of Chandra Prabha Prakhand, Pt. D.D.U. Nagar, CDL. Their invaluable support in providing all necessary data for the Left Karmanasa Canal System was essential for conducting this research study. I am also grateful for the opportunity to visit the site, which enhanced understanding of the system through the information provided by these individuals.

Data Availability Statement

The datasets generated during the current study are available from the corresponding author on reasonable request.

Conflict of Interest

The authors declare that they have no known competing financial interests or personal relationships that could have appeared to influence the work reported in this paper.

Funding

This research received no external funding.

References

Abo-Sreeaa, D. A., AboulAtta, N. M. and El-Molla, D. A. 2023. The impact of blockage on the performance of canal coverage structures. Journal of Engineering and Applied Science, 70: 76. https://doi.org/10.1186/s44147-023-00246-0

Ardıçlıoğlu, M. and Kuriqi, A. 2019. Calibration of channel roughness in intermittent rivers using HEC-RAS model: Case of Sarimsakli Creek, Turkey. Applied Sciences, 1: 1080. https://doi.org/10.1007/s42452-019-1141-9

ASCE Task Committee on Definition of Criteria for Evaluation of Watershed Models. 1993. Criteria for evaluation of watershed models. Journal of Irrigation and Drainage Engineering, 119: 429–442. https://doi.org/10.1061/ASCE0733-

94371993119:3429

Barkhordari, S. and Shahdany, S. 2022. A systematic approach for estimating water losses in irrigation canals. Water Science and Engineering, 15: 161–169. https://doi.org/10.1016/j.wse.2022.02.004

Bwambale, E., Home, P., Raude, J. and Wanyama, J. 2019. Hydraulic performance evaluation of the water conveyance system of Doho Rice Irrigation Scheme in Uganda, 101–112.

Chow, V. T. 1959. Open channel hydraulics. McGraw-Hill.

Clarke, D., Andrews, P., Meseth, E., Sala, R. and Deom, J. 2010. Analysis of the hydraulics of the irrigation canals of Otrar, Kazakhstan. Water Science and Technology: Water Supply. https://doi.org/10.2166/ws.2010.114

Gilja, G., Harasti, A. and Fliszar, R. 2021. DrainCAN—A MATLAB function for generation of a HEC-RAS-compatible drainage canal network model. Computation, 9: 51. https://doi.org/10.3390/computation9050051

Goodell, C. 2016. Advanced gate operation strategies in HEC-RAS 5.0. In Crookston, B. & Tullis, B. (Eds.), Hydraulic Structures and Water System Management: 6th IAHR International Symposium on Hydraulic Structures, 519–527. https://doi.org/10.15142/T3430628160853

Gruss, L., Glowski, R. and Wiatkowski, M. 2018. Modeling of water flows through a designed dry dam using the HEC-RAS program. ITM Web of Conferences, 23: 00012. https://doi.org/10.1051/itmconf/20182300012

Kamran, M., Yousaf, W., Rajapakse, L., Awan, W., Riaz, M., Asif, N., Umar, M. and Shah, U. 2020. Innovative initiative for effective operation and monitoring using HEC-RAS modelling of Hakra Branch Canal System, Pakistan. Irrigation and Drainage, 70: 1–15. https://doi.org/10.1002/ird.2524

Legates, D. and McCabe, G. 1999. Evaluating the use of goodness-of-fit measures in hydrologic and hydroclimatic model validation. Water Resources Research, 35: 233–241. https://doi.org/10.1029/1998WR900018

Mohammed, J. R. and Qasim, J. M. 2012. Comparison of one-dimensional HEC-RAS with two-dimensional ADH for flow over trapezoidal profile weirs. Caspian Journal of Applied Sciences Research, 1: 1–12.

Moriasi, D., Arnold, J., Liew, M., Bingner, R., Harmel, R. and Veith, T. 2007. Model evaluation guidelines for systematic quantification of accuracy in watershed simulations. Transactions of the ASABE, 50. https://doi.org/10.13031/2013.23153

Nash, J. E. and Sutcliffe, J. V. 1970. River flow forecasting through conceptual models: Part I. A discussion of principles. Journal of Hydrology, 10: 282–290.

Nugroho, E. P., Niiam, M. F. and Soedarsono, S. 2021. Technical review of operational patterns of the West Flood Channel Movement in Semarang City. Journal of Industrial Engineering and Management Research, 2: 291–299.

Ontowirjo, B., Fathurrahman, I., Ramadhan, M. V., Zahriani, A., Zahra, M. and Wahyudi, H. 2023. LiDAR DEM and HEC-RAS On-Grid Rainfall Hydrograph Model for irrigation system. IOP Conference Series: Earth and Environmental Science, 1198: 012023.

Parhi, P., Sankhua, R. and Roy, G. 2012. Calibration of channel roughness for Mahanadi River, India, using HEC-RAS model. Journal of Water Resource and Protection, 4: 847–850. https://doi.org/10.4236/jwarp.2012.410098

Patamanska, G. and Grancharova, E. 2019. Hydraulic modeling for better operational performance of existing irrigation canal. Acta Technica Corviniensis – Bulletin of Engineering, 12: 107–110.

Prakash, K., Rawat, D., Singh, S., Chaubey, K., Kanhaiya, S. and Mohanty, T. 2019. Morphometric analysis using SRTM and GIS: A case study of the Karmanasa River Basin, North Central India. Applied Water Science, 9: 1–10. https://doi.org/10.1007/s13201-018-0887-3

Santhi, C., Arnold, J. G., Williams, J. R., Dugas, W. A., Srinivasan, R. and Hauck, L. M. 2001. Validation of the SWAT model on a large river basin with point and non-point sources. Journal of the American Water Resources Association, 37; 1169–1188.

Sargison, J. E. and Barton, A. F. 2008. Application of HEC-RAS to hydraulic modelling of an irrigation scheme to determine potential for capacity increase. 9th National Conference on Hydraulics in Water Engineering.

Serede, I. J., Mutua, B. M. and Raude, J. M. 2015. Calibration of channel roughness coefficient for Thiba Main Canal Reach in Mwea

Irrigation Scheme, Kenya. Hydrology, 3: 55–65.

Timbadiya, P. V., Patel, P. L. and Porey, P. D. 2011. Calibration of HEC-RAS model for prediction of flood for Lower Tapi River, India. Journal of Water Resource and Protection, 3: 805–811.

Uttar Pradesh Irrigation and Water Resource Department. 1823. Chandraprabha Division Pt. D. D. U. Nagar, Chandauli office. https://idup.gov.in/en/

Vedmani, Panda, R. K. and Pandey, V. K. 2020. Calibration and validation of HEC-RAS model for minor command in coastal region. International Journal of Current Microbiology and Applied Sciences, 9: 664–678. https://doi.org/10.20546/ijcmas.2020.902.082

About District Chandauli. 2024. Government of Uttar Pradesh. https://chandauli.nic.in/about-district/

Geography, District Chandauli. 2024. Government of Uttar Pradesh. https://chandauli.nic.in/geography/

India WRIS. 2024. https://indiawris.gov.in/wris

NASA POWER. 2024. https://power.larc.nasa.gov